Assessing methane emissions for northern peatlands in ORCHIDEE-PEAT revision 7020.

Elodie Salmon[1], Fabrice Jégou[1], Bertrand Guenet[2,3], Line Jourdain[1], Chunjing Qiu[2], Vladislav Bastrikov[4], Christophe Guimbaud[1], Dan Zhu[2,5], Philippe Ciais[2], Philippe Peylin[2], Sébastien Gogo[6], Fatima Laggoun-Défarge[6], Mika Aurela[7], M. Syndonia Bret-Harte[8], Jiquan Chen[9], Bogdan H. Chojnicki[10], Housen Chu[11], Colin W. Edgar[8], Eugenie S. Euskirchen[8], Lawrence B. Flanagan[12], Krzysztof Fortuniak[13], David Holl[14], Janina Klatt[15], Olaf Kolle[16], Natalia Kowalska[17], Lars Kutzbach[14], Annalea Lohila[7], Lutz Merbold[18], Włodzimierz Pawlak[13], Torsten Sachs[19], Klaudia Ziemblińska[20].

[1]Laboratoire de Physique et Chimie de l'Environnement et de l'Espace, LPC2E, 45071, Orléans cedex 2, France.
[2]Laboratoire des Sciences du Climat et de l'Environnement, UMR8212, CEA-CNRS-UVSQ F-91191 Gif sur Yvette, France.
[3] Laboratoire de Géologie de l'ENS, IPSL, CNRS, PSL Research University, Laboratoire de Géologie de l'ENS, 24 rue Lhomond, 75231 Paris cedex 05, France.
[4]Science Partners, 75010 Paris, France.
[5] Sino-French Institute for Earth System Science, College of Urban and Environmental Sciences, Peking University, Beijing, China.
[6] Institut des Sciences de la Terre d'Orléans, Université d'Orléans, CNRS, BRGM, UMR 7327, 45071 Orléans, France.
[7] Finnish Meteorological Institute, Climate Research Programme, Helsinki, Finland
[8] Institute of Arctic Biology, University of Alaska Fairbanks, Fairbanks, AK, USA.
[9] Landscape Ecology & Ecosystem Science (LEES) Lab, Department of Geography, Environment, and Spatial Sciences, & Center for Global Change and Earth Observations, Michigan State University, East Lansing, MI 48823
[10] Laboratory of Bioclimatology, Department of Ecology and Environmental Protection, Faculty of Environmental Engineering and Mechanical Engineering, Poznan University of Life Sciences, Piątkowska 94, 60-649 Poznań, Poland
[11] Climate and Ecosystem Sciences Division, Lawrence Berkeley National Lab, USA, 1 Cyclotron Rd, Berkeley, CA 94720
[12] Department of Biological Sciences, University of Lethbridge, 4401 University Drive, Lethbridge, Alberta, Canada
T1K 3M4
[13] Department of Meteorology and Climatology, Faculty of Geographical Sciences, University of Lodz, Lodz, Poland
[14] Institute of Soil Science, Center for Earth System Research and Sustainability (CEN), Universität Hamburg, Hamburg, Germany
[15] Weihenstephan-Triesdorf University of Applied Sciences, Institute of Ecology and Landscape,Chair of Vegetation Ecology, Am Hofgarten 1, 85354 Freising, Germany
[16] Field Experiments and Instrumentation, Max-Planck-Institute for Biogeochemistry,Hans-Knoell-Strasse 10, D-07745 Jena, Germany
[17] Department of Matter and Energy Fluxes, Global Change Research Institute, Czech Academy of Sciences, Bělidla 986/4a, 603 00 Brno, Czech Republic.
[18] Department Agroecology and Environment, Agroscope, Reckenholzstrasse 191, 8046 Zurich, Switzerland
[19] GFZ German Research Centre for Geosciences, Telegrafenberg, Potsdam, Germany,
[20] Laboratory of Meteorology, Department of Construction and Geoengineering, Faculty of Environmental Engineering and Mechanical Engineering, Poznan University of Life Sciences, Piątkowska 94, 60-649 Poznań, Poland.

Correspondence to: Elodie Salmon (elodie.salmon@cnrs-orleans.fr)

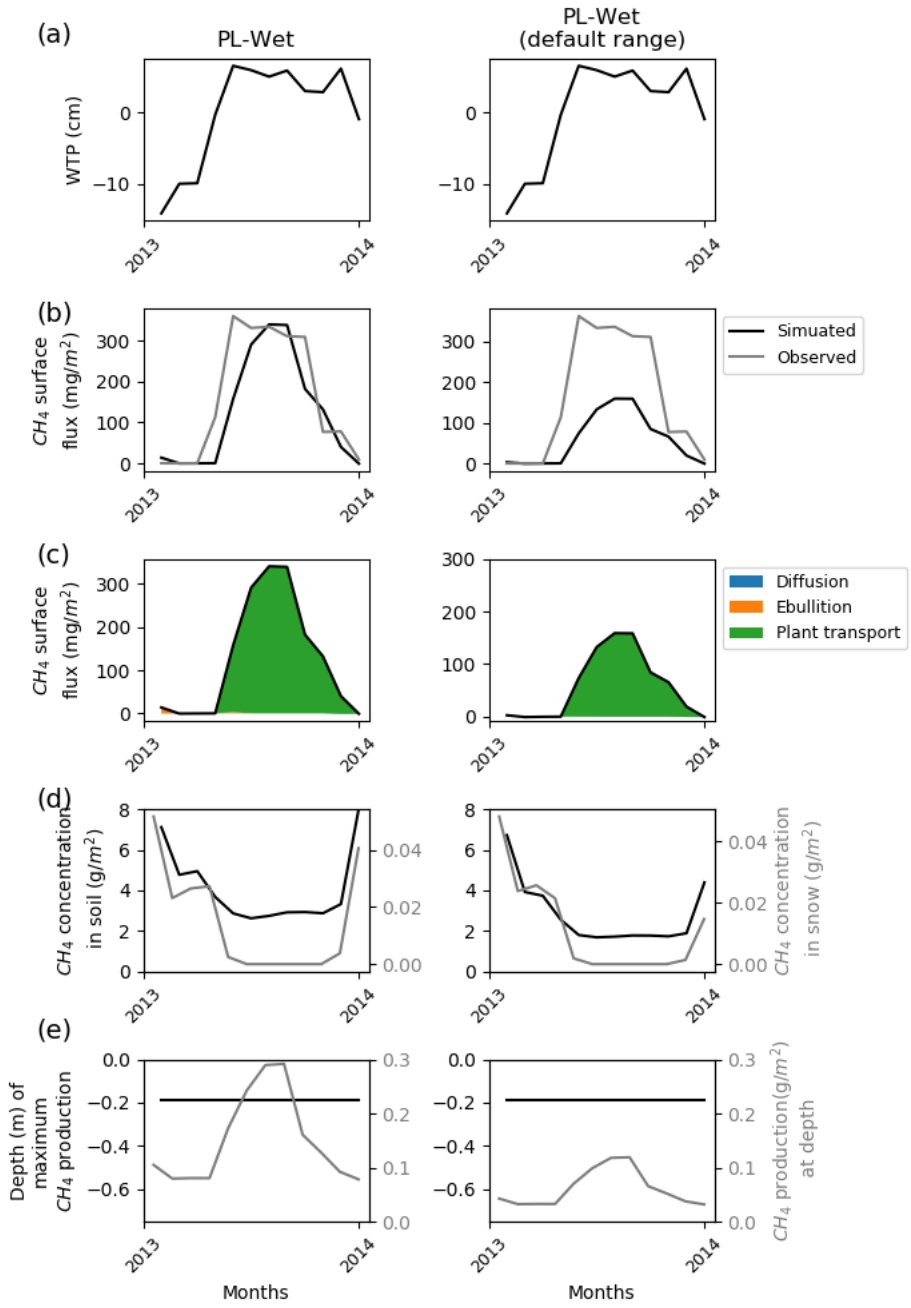

Fig.S1. Temporal distribution of methane at PL-Wet using optimized parameters (see Table S1) defined from an extended range (right) and from the default range (left). (a) Simulated water table position estimated from the soil water content; (b) Simulated (dark line) and observed (gray line) methane emissions released to the atmosphere; (c) Cumulative amount of methane emitted by diffusion, plant mediated transport and ebullition; (d) Methane concentration in the soil layers (dark line) and in the snow layers (gray line); (e) On the left, depth at which methane production is the highest in the soil, scaled to the maximum peat depth. On the right, amount of methane produced at these depths.

Table S1. Single site prior and optimized values of methane scheme parameters for PL-Wet. Discrepancies between methane emissions observed and simulated are quantify by the root mean square difference (RMSD). Minimization efficiency of each test are indicated by the relationship between the prior using default values and posterior RMSD: (1 - RMSDpost / RMSDprior)x100.

		PL-Wet A		PL-Wet (default range)	
Parameters	Units	prior	post	prior	post
q_{MG}	proportion	10.0 (1.0, 11.0)	4.0	10.0	9.8
k_{MT}	1/s	1.3	2.0	1.3	1.5
M_{rox}	fraction	0.5	0.165	0.5	0.030
Z_{root}	m	0.3	0.328	0.3	0.330
T_{veg}	proportion	5.0	6.0	7.0	7.4
wsize	m	0.01	0.0110	0.01	0.0111
mxr_{CH4}	fraction	0.15	0.136	0.25	0.244
RMSD		183.0	80.5	267.6	227.4
$1-(RMSD_{post}/RMSD_{prior})$	%		56.04		15.02

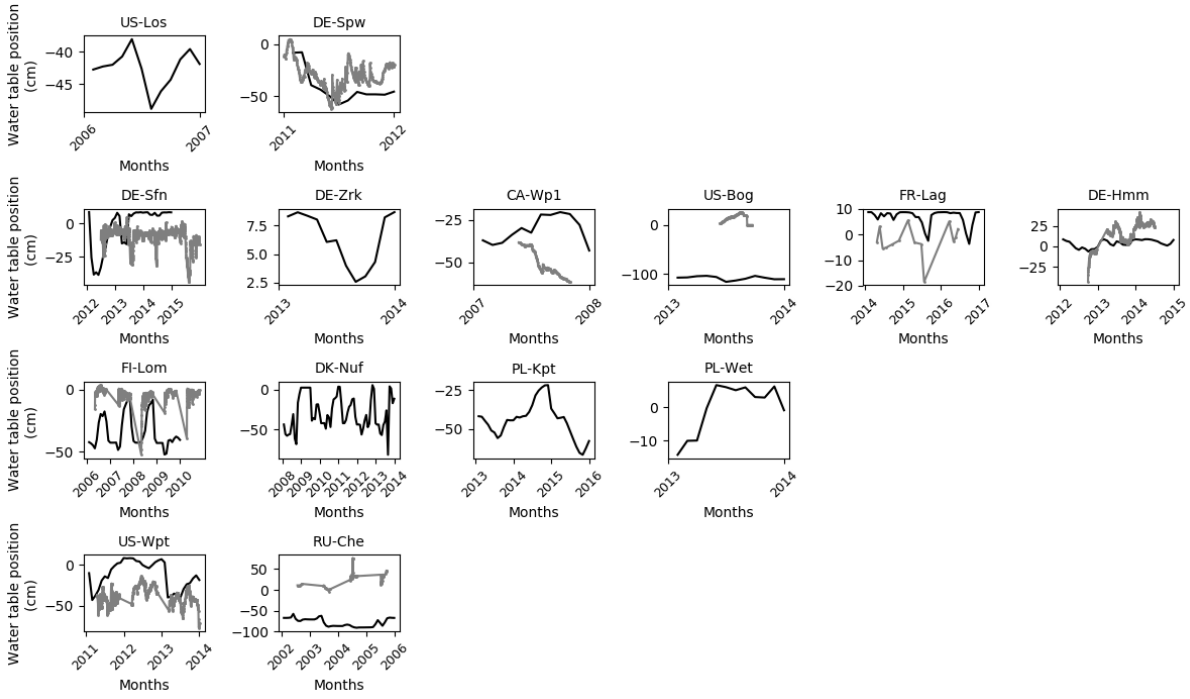

Fig. S2: Simulated (dark line) and observed (gray line) water table position.

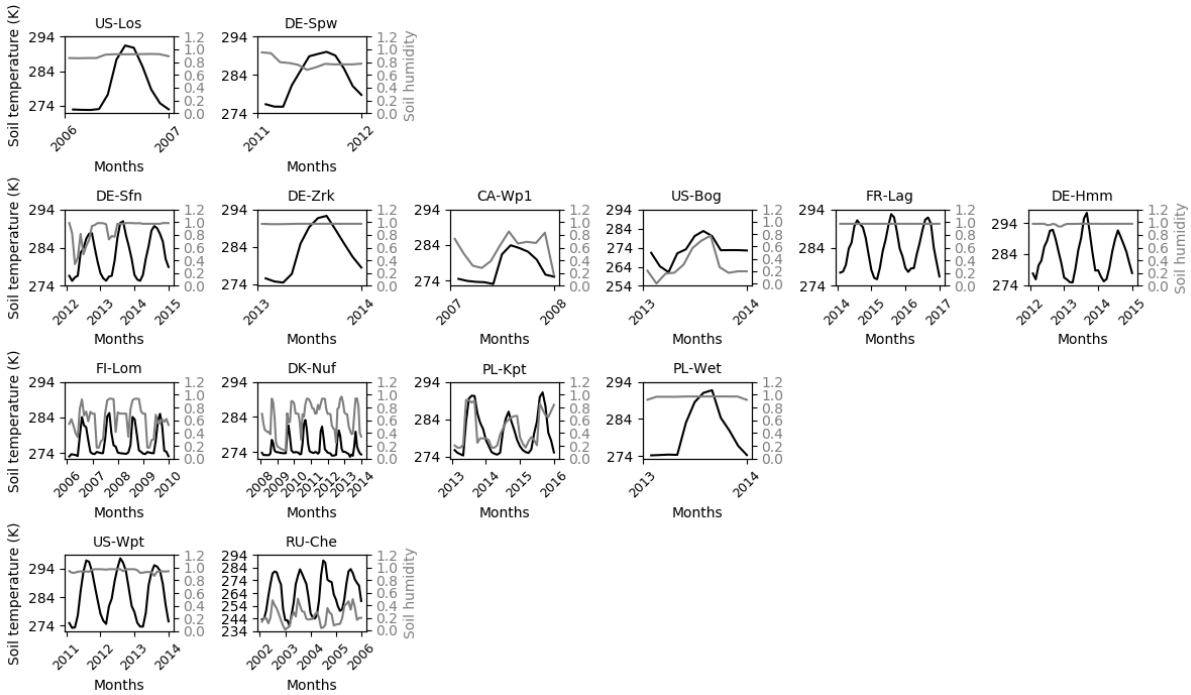

Fig. S3: Soil temperature (dark line) and soil humidity (gray line) at the depth of maximum methane production.

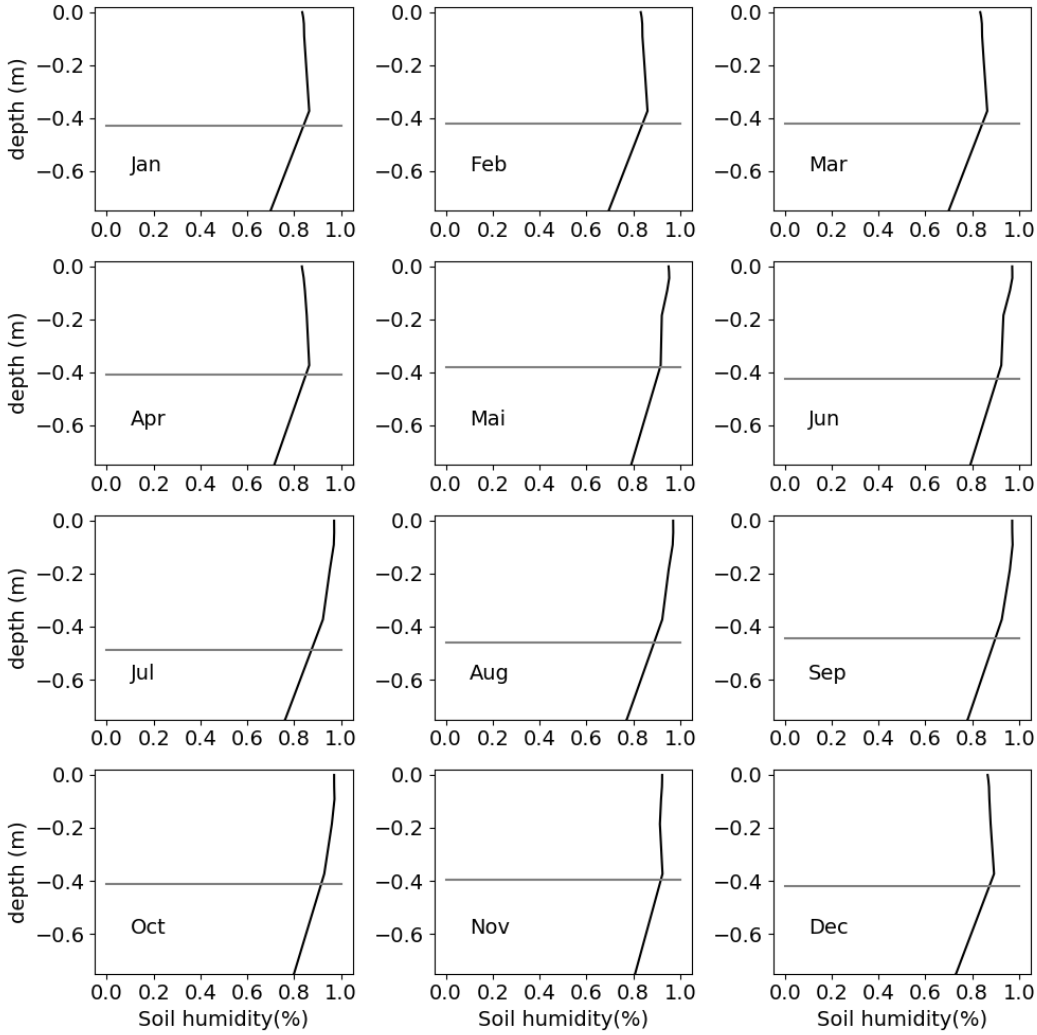

Fig. S4: Monthly soil humidity profiles (solid line) and water table position (grey line) at US-Los.

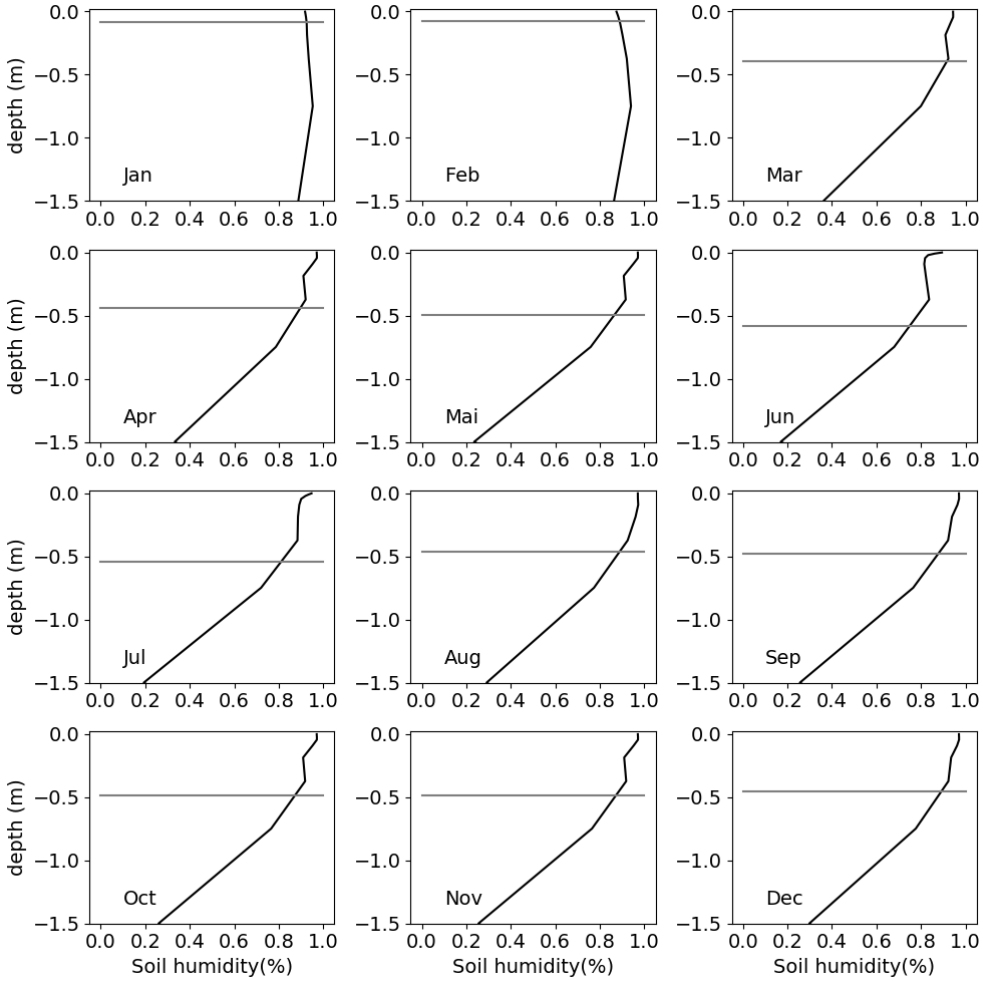

Fig. S5: Monthly soil humidity profiles (solid line) and water table position (grey line) at DE-Spw.

Table S2. Root mean square difference (RMSD) of the first optimization prior and the last optimization posterior. The relationship between the prior using default values and posterior RMSD: (1 - RMSDpost / RMSDprior)100 indicates minimization efficiency of the successive optimization runs.

Sites identifiation	RMSDprior	RMSDpost	1-($RMSD_{post}$/$RMSD_{prior}$)
			%
US-Los	69.6	1.1	98.44
DE-spw	687.9	9.5	98.62
DE-Sfn	263.3	9.2	96.50
DE-Zrk	16.2	4.6	71.44
CA-Wp1	73.6	11.8	84.03
US-Bog	33.0	6.7	79.82
FR-Lag	91.4	23.0	74.86
DE-Hmm	34.4	25.3	26.34
FI-Lom	44.0	38.3	12.93
DK-NuF	44.6	40.1	9.97
PL-Kpt	146.5	54.6	62.70
PL-Wet	181.3	80.5	55.63
US-Wpt	265.5	249.0	6.21
RU-che	157.4	139.7	11.25

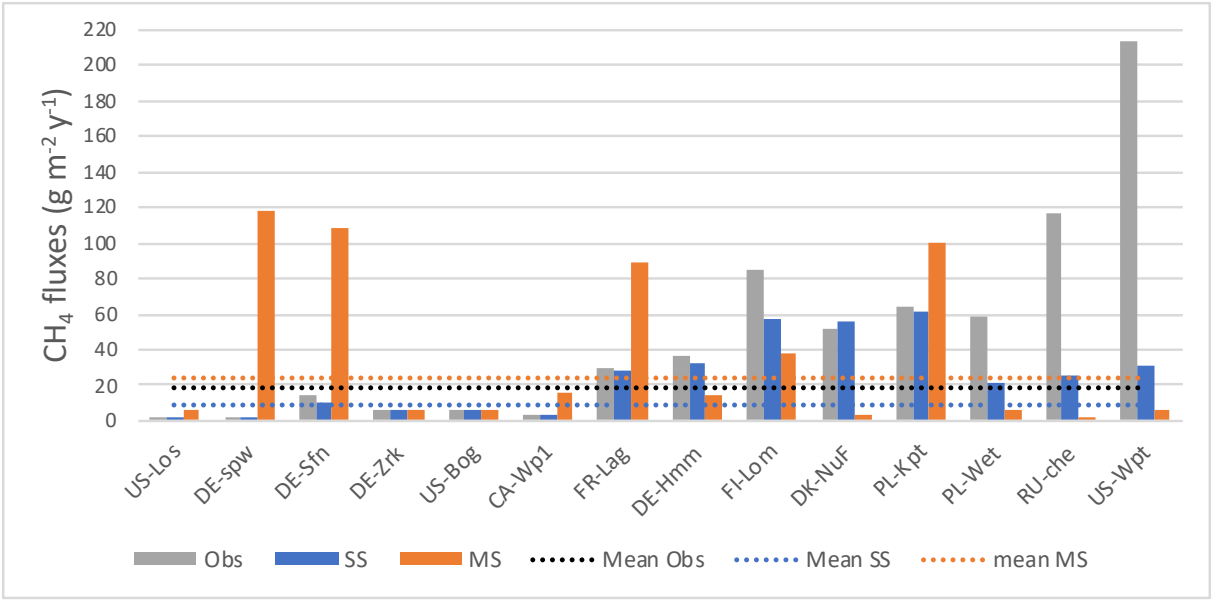

Fig. S6: Annual methane emissions defined from the observed data (Obs in grey), from simulations employing optimized parameters obtained by the single site optimization (SS in blue) and by multi-site optimization (MS in orange). Dotted lines indicate the mean values of annual methane fluxes across sites.

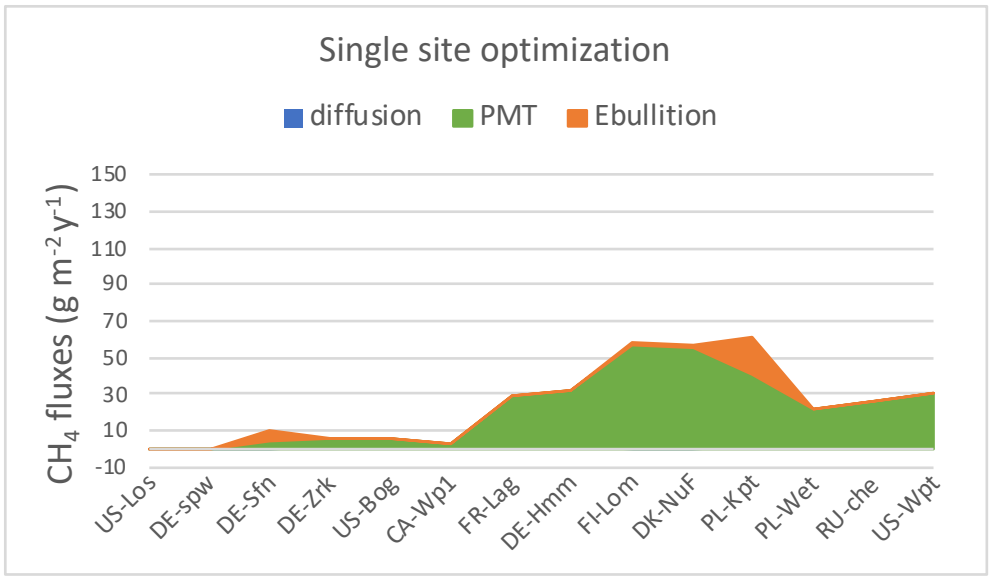

Fig. S7: Stacked area of annual methane fluxes by type of transport process, diffusion, plant mediated transport (PMT) and ebullition for the single site optimization simulations.

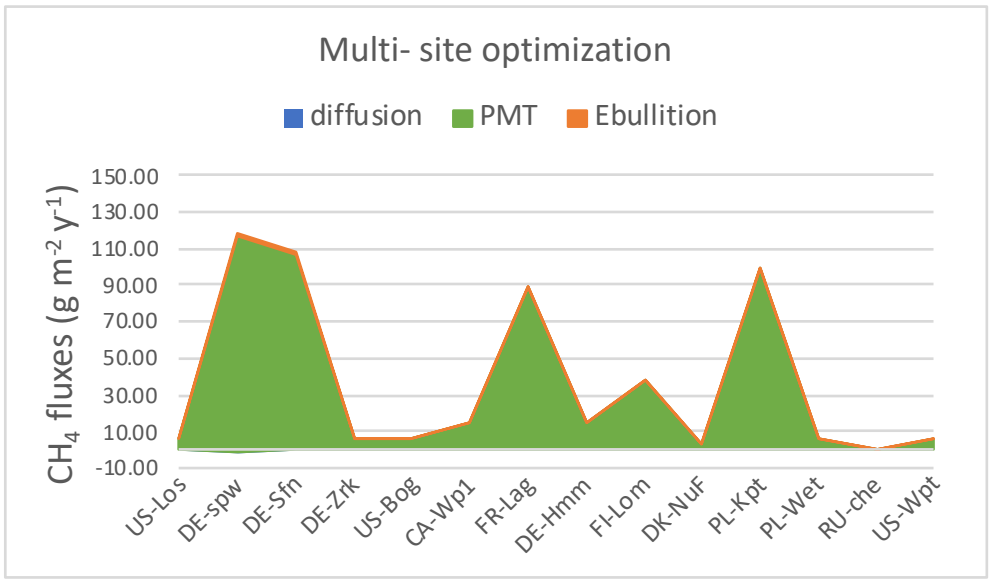

Fig. S8: Stacked area of annual methane fluxes by type of transport process, diffusion, plant mediated transport (PMT) and ebullition for the multi-site optimization simulations.

Table S3. Multi-site prior using extended ranges and optimized values of methane scheme parameters. Parameters description and references are in Table3.

Parameters	Unit	Prior values	Prior ranges	Posterior values
q_{MG}	proportion	9.28	1.0, 11.0	7.63
k_{MT}	1/d	2.59	1.0, 8.1	3.80
M_{rox}	fraction	0.44	0.0, 1.0	0.76
Z_{root}	m	0.27	0.01, 0.5	0.25
T_{veg}	proportion	6.99	0.0, 40.0	12.16
wsize	m	0.0088	0.001, 0.1	0.0010
mxr_{CH4}	fraction	0.24	0.05, 0.75	0.25

Table S4. Evaluation of gaps between methane emissions observed and simulated of single site ($RMSD_{SS}$) and multi-site ($RMSD_{MS}$) optimizations. Minimization efficiency of each test are indicated by the relationship between the RMSD from the single site simulation and RMSD obtained for the multi-site simulation.

	$RMSD_{SS}$	$RMSD_{MS}$	$RMSD_{MS}$ / $RMSD_{SS}$
US-Los	1.1	36.55	33.7
DE-spw	9.5	345.9	36.4
DE-Sfn	9.2	134.10	14.6
DE-Zrk	4.6	4.91	1.1
US-Bog	6.7	19.44	2.9
CA-Wp1	11.8	44.12	3.8
FR-Lag	23.0	41.22	1.8
DE-Hmm	25.3	10.1	0.4
FI-Lom	38.3	48.59	1.3
DK-NuF	40.1	44.79	1.1
PL-Kpt	54.6	65.79	1.2
PL-Wet	80.5	174.30	2.2
RU-che	139.7	157.80	1.1
US-Wpt	249.0	273.10	1.1

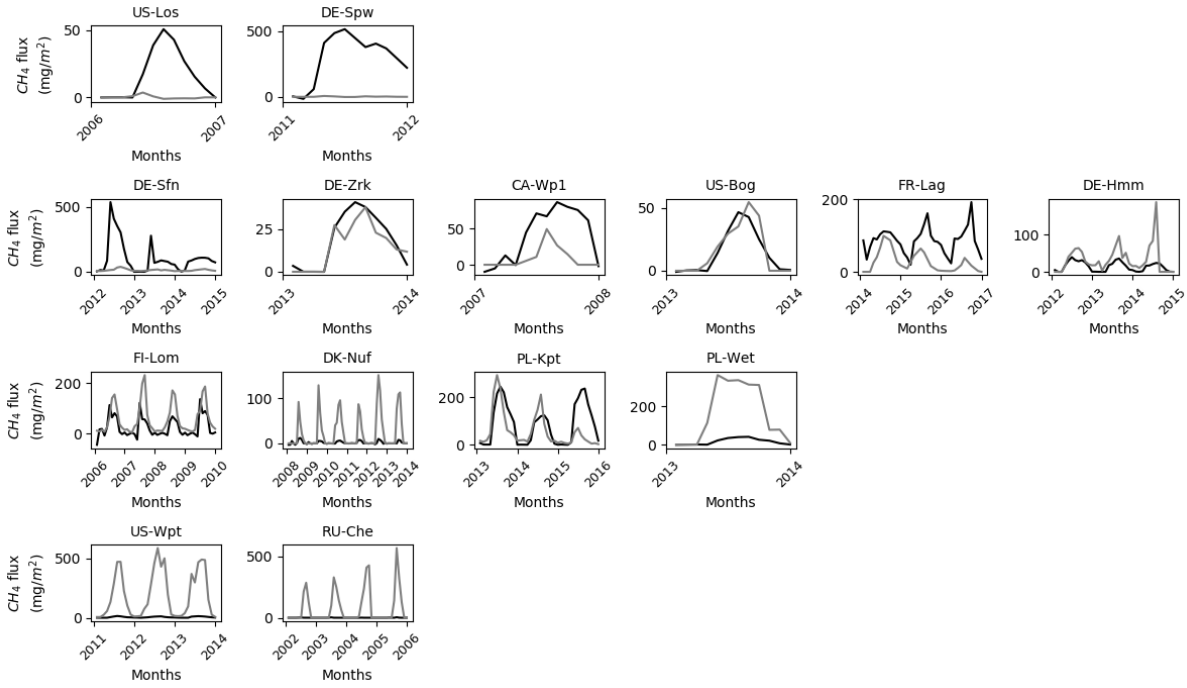

Fig. S9: Simulated (dark line) and observed (gray line) methane emissions using multi-site optimized parameters obtained with extended ranges values defined in Table S3.

Table S5. Annual methane emissions defined from the observed data (Obs), from simulations employing optimized parameters obtained by the single site optimization (SSO) and by multi-site optimization (MSO)using the extended range. The methane fluxes combine methane emitted by diffusion, plant mediated transport and ebullition.

Site	Data	CH_4 fluxes	Diffusion	Plant mediated transport	Ebullition
		g m^{-2} y^{-1}	g m^{-2} y^{-1}	g m^{-2} y^{-1}	g m^{-2} y^{-1}
US-Los	Obs	0.05			
	SSO	0.01	0.003	0.01	0.0
	MSO	6.07	-0.01	6.08	0.0
DE-spw	Obs	0.46			
	SSO	0.07	-0.29	0.34	0.02
	MSO	109.51	-0.50	107.32	2.70
DE-Sfn	Obs	14.01			
	SSO	9.63	-0.22	5.03	4.82
	MSO	110.11	-0.19	103.46	6.84
DE-Zrk	Obs	5.60			
	SSO	5.68	-0.001	5.53	0.15
	MSO	6.74	-0.002	6.63	0.11
US-Bog	Obs	5.74			
	SSO	5.48	0.05	5.44	0.0
	MSO	5.26	0.04	5.22	0.0
CA-Wp1	Obs	3.29			
	SSO	3.19	-0.12	3.12	0.19
	MSO	14.74	-0.11	14.84	0.01
FR-Lag	Obs	9.91			
	SSO	9.57	-0.01	9.58	0.0005
	MSO	31.40	-0.003	31.32	0.0747
DE-Hmm	Obs	12.19			
	SSO	10.77	-0.0015	10.68	0.09
	MSO	5.11	-0.0001	5.06	0.05
FI-Lom	Obs	21.15			
	SSO	14.48	-0.23	14.60	0.110
	MSO	9.14	0.05	9.08	0.002
DK-NuF	Obs	8.69			
	SSO	9.42	-0.05	9.21	0.26
	MSO	1.82	-0.03	1.50	0.35
PL-Kpt	Obs	21.22			
	SSO	20.35	-0.03	13.78	6.61
	MSO	30.95	-0.04	30.89	0.10
PL-Wet	Obs	58.96			
	SSO	21.31	-0.042	21.25	0.096
	MSO	5.82	0.001	5.81	0.002
RU-che	Obs	38.92			
	SSO	8.46	-0.0001	8.46	0.0
	MSO	0.17	-0.0006	0.17	0.0
US-Wpt	Obs	53.40			
	SSO	7.61	0.0	7.61	0.0
	MSO	1.45	0.0	1.45	0.0

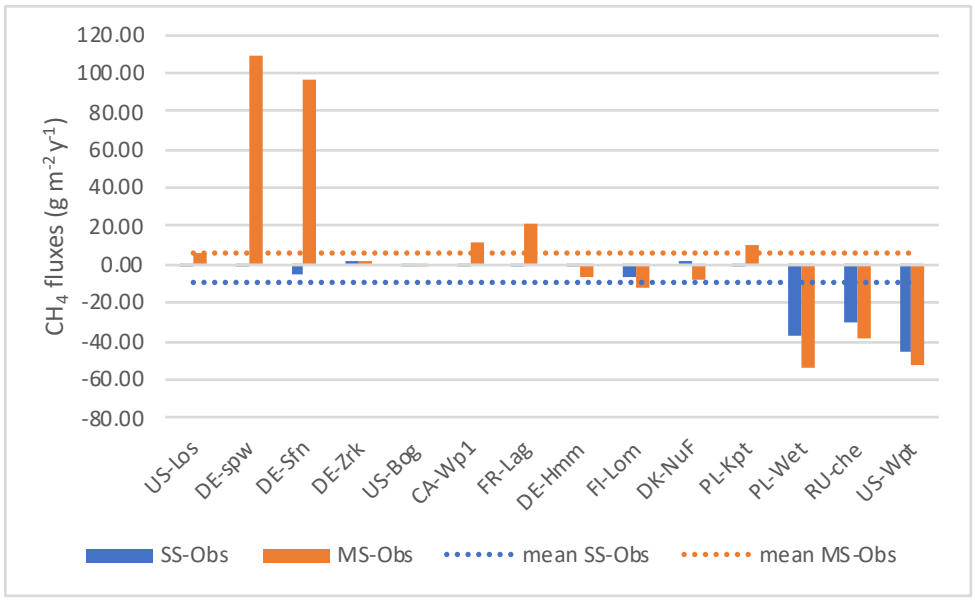

Figure S10: Difference in annual methane emissions between the observed data (Obs), and simulations employing optimized parameters obtained by the single site optimization (SSO) and by multi-site optimization (MSO) using the extended range.